

# PREPARATION AND CHARACTERIZATION OF MAGNETIC Fe, Fe/C AND Fe/N NANOPARTICLES SYNTHESIZED BY CHEMICAL VAPOR CONDENSATION PROCESS

Chul-Jin Choi<sup>1</sup>, Byoung-Kee Kim<sup>1</sup>, Oleg Tolochko<sup>2</sup> and Li-Da<sup>3</sup>

<sup>1</sup> Korea Institute of Machinery and Materials, 66 Sangnam-Dong, Changwon, Kyungnam 641-010, Korea

<sup>2</sup> Material Science Faculty, State Technical University, 195251, Saint Petersburg, Russia,

<sup>3</sup>Shenyang National Laboratory for Materials Science and International Center for Materials Physics, Institute of Metal Research, Chinese Academy of Sciences, Wenhua Road 72, Shenyang, 110016, PR China

Received: June 25, 2003

**Abstract.** Nano-sized Fe, Fe/C and Fe/N particles had been synthesized by Chemical Vapor Condensation (CVC) process and studied by means of HRTEM, XRD and vibration sample magnetometer. The precursor of iron carbonyl ( $\text{Fe}(\text{CO})_5$ ) was used as a source of metallic vapor and carbon monoxide or ammonium gas – as the sources of carbon or nitrogen. As-prepared nanoparticles had nearly spherical shape and core-shell type structure. The influence of experimental parameters on structure and phase composition of nanoparticles was investigated. With the precursor decomposition temperature increase, the particle size increased and size distribution changed from symmetric to asymmetric one. The main phase of Fe/C nanoparticles shifted from  $\text{Fe}_3\text{C}$  to  $\alpha$ -Fe with the change of reaction temperature and carrier gas flow rate. The core/shell structure of iron oxide-coated Fe/N nanoparticles correlated with the experimental parameters of the CVC process, which strongly affected their magnetic properties.

## 1. INTRODUCTION

As a new branch of materials research, nanoparticles have been attracting a great deal of attention because of their potential applications in areas such as electronics, optics, catalysis, ferrofluids, and magnetic data storage [1-3]. Their unique properties and the improved performances are determined by their particle sizes, surface structures and inter-particle interactions.

Nanoparticles have been prepared by different methods, such as arc-discharge [4], mechanical alloying [5], hydrogen plasma-metal reaction [6], inert gas condensation [7] and chemical vapor condensation (CVC) [8,9]. All those methods have some limitations, however, as compared with other ones, CVC method has been developed for preparation of almost all kinds of materials since a wide range of precursors are commercially available;

moreover, CVC method can usually produce a large amount of nanoparticles.

In the present work, we synthesized Fe, Fe/C and Fe/N nanoparticles by Chemical Vapor Condensation (CVC) method from organometallic precursor of iron pentacarbonyl ( $\text{Fe}(\text{CO})_5$ ). The structural and magnetic properties of free-standing nanoparticles were investigated.

## 2. EXPERIMENTAL DETAILS

The basic setup for CVC is similar to that described in literature elsewhere [10]. To produce iron nanoparticles, various carrier gases such as Ar, He, CO and  $\text{NH}_3$  are fed through a heated bubbling units containing the liquid iron pentacarbonyl ( $\text{Fe}(\text{CO})_5$ ) precursor. The flow of the carrier gas entrains precursor vapor and pass through the heated tubular furnace in which the precursor pyrolyzes and con-

---

Corresponding authors: Chul-Jin Choi, e-mail: cjchoi@kmail.kimm.re.kr; Oleg Tolochko, e-mail: oleg@ispm.hop.stu.neva.ru

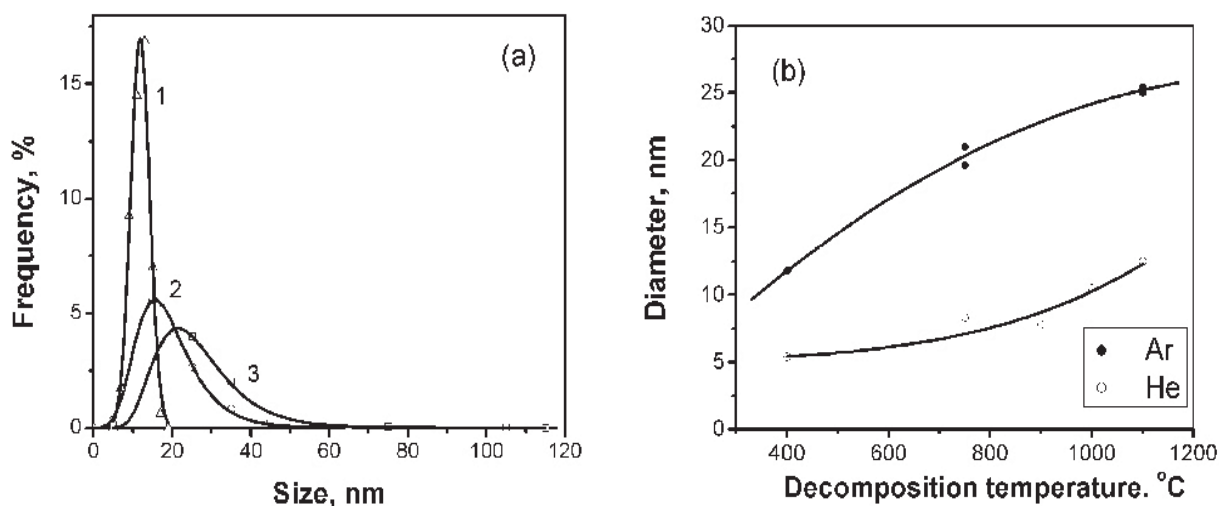


**Fig. 1.** Particle size distributions (a) and median particle diameter (b) versus precursor decomposition temperature for iron nanoparticles, which were synthesized using argon or helium as a carrier gas.

denses into clusters or particles. The synthesized powders are scraped off and collected from a rotating chiller cooled by liquid nitrogen. Experiments were conducted with a tubular furnace uniformly heated at a temperature between 400 and 1100 °C.

The morphology, size and lattice images of particles were determined with HRTEM (High Resolution Transmission Electron Microscopy). The powder for TEM investigations was ultrasonically dispersed in ethanol and dropped on a carbon coated copper grid. Identification of the phases in the samples was carried out in X-ray diffractometer with  $\text{CuK}_\alpha$  radiation. Magnetization was measured by a vibrating sample magnetometer (VSM) at room temperature in a field up to 20 kOe.

### 3. RESULTS AND DISCUSSION

#### 3.1. Pure Fe nanoparticles

All Fe nanoparticles consist of dark core and light shell. The particle shape is nearly spherical. The core is metallic and shell is composed of metal oxides [11]. The shell thickness is about 3-4nm irrespective of particle size. Fig.1a presents the normalized size distributions for particles prepared at decomposition temperatures of 400, 750, and 1100 °C using argon as a carrier gas. Figs. 1a and 1b show that the mean particle size decreases with decrease in the precursor decomposition temperature. At the decomposition temperature of 400 °C,

particles have a minimal size and actually symmetric size distribution, at the lower temperatures powders could not be synthesized. As the decomposition temperature increased, the distribution became wider and more asymmetric. The increasing of saturation vapor pressure with an increase of the decomposition temperature can enhance the growth of nucleus, which results in the larger particle formation. Also the high kinetic energy of gas molecules and as-formed iron particles in the gas phase can lead to the increasing in number of collision between the particles and consequently, to the preferable growth of larger ones.

The increase of median particle diameter at increasing decomposition temperature in argon and helium atmosphere is shown in the Fig.1b. The size of particles prepared under helium atmosphere is significantly smaller, probably due to the higher mobility and heat conductivity of He, which lead to more rapid cooling of particles in the environment of He gas as compared with Ar.

If particle size increases above 8nm, the crystalline X-ray patterns of BCC solid solution can be detected, and thus allows lattice parameter calculations. The measured values of lattice constant are larger than that of pure iron ( $a_{\text{BCC-Fe}}=2.8664 \text{ \AA}$ ) and increase with decreasing particle size. Dependence of lattice constant on average particle size can be explained by the interaction between the metallic core and oxide shell if the growth of oxide is as-

**Table 1.** Phase composition of Fe/C nanoparticles with CO/Ar ratio.

Temperature	Carrier gas	Gas flow rate, cc/min	Phase composition	Particle size, nm
400	CO	400	BCC-Fe+Fe <sub>3</sub> C (trace)	20-50
		800	BCC-Fe	15-35
500	CO	400	Fe <sub>3</sub> C	20-100
		800	BCC-Fe+Fe <sub>3</sub> C	20-70
		1200	BCC-Fe	15-50
600	CO + Ar (1:3)	800	BCC-Fe + oxides	
	CO	<1600	Fe <sub>3</sub> C	15 - 100
		2400	BCC-Fe+Fe <sub>3</sub> C	15-55
700	CO	4000	BCC-Fe	14-30
		<2400	Fe <sub>3</sub> C	
		800	BCC-Fe+Fe <sub>3</sub> C	50-170
900	CO+Ar (1:1)	800	BCC-Fe+Fe <sub>3</sub> C	
1000	CO+Ar (1:3)	800	BCC-Fe+Fe <sub>3</sub> C (trace)	
1100	CO	400-800	Fe <sub>3</sub> C	
800		Fe <sub>3</sub> C		
<1000		BCC + FCC Fe + Fe <sub>3</sub> C	40-350	
1100	CO	2400	Fe <sub>3</sub> C	30 - 150
		800	BCC + FCC Fe	70-250

sumed to be epitaxial. K.K. Fung *et al.* [12] also showed that the epitaxial growth of oxide shell on the iron nanoparticles has a lattice misfit of about 3%. That can lead to compressive stresses induced in oxide shell and tensile stresses in metallic core, which causes increasing lattice constant in oxide-coated nanoparticles. Another possible reason for lattice parameter increasing is the influence of dissolved interstitial atoms. The admixtures of interstitial atoms such as carbon or oxygen can be introduced in the lattice of iron particles during their formation by the vapor condensation and then fixed by subsequent rapid quenching (estimated cooling rate in CVC process is about 10<sup>6</sup> K/sec [13]). The second reason can cause a general increase of lattice constant, which is independent of particle size.

### 3.2. Fe/C nanoparticles

Carbon monoxide (CO) was used as a carrier gas and as the source of carbon to prepare iron – carbon alloyed nanoparticles. Under the high temperature conditions and in the presence of metallic catalyst (Fe, Ni, Co etc) CO gas undergo a disproportionation by the reaction:  $2\text{CO} = \text{CO}_2 + \text{C}$ ,  $\Delta H = -171$  kJ/mol. That reaction is of great value for different metallurgical processes and already had been investigated in detail [14]. The reaction is thermodynamically prohibited at temperatures higher than about 900 °C (CO and CO<sub>2</sub> equilibrium composition

is 97% and 3%, respectively). This means that, at higher temperatures, the reaction of CO disproportionation is likely to occur in the tubular furnace either before or after the high temperature zone of reactor, when the local temperature is lower than about 900 °C. Moreover, kinetic investigations [14] of carbon monoxide disproportionation on the surface of high porosity nickel showed that the appreciable reaction rates were in the temperature interval from 520 to 800 °C with maximum rate at a temperature of 670 °C. However, kinetics of that reaction also strongly depend on properties of catalyst.

The results of the experiments, which were carried out at different process parameters are shown in the Table 1. By variation of the experimental parameters it is possible to obtain different phase composition and particle size. X-ray diffraction analysis of nanoparticles (Fig. 2) shows that in the temperature region of 500-1000 °C the fully cementite particles can be obtained at the lowest CO flow rate. It means that temperature and residential time in the decomposition furnace are enough for full reaction between free carbon on metallic surface and iron of particles. The decreasing temperature lead to the formation of BCC iron phase, which appears in the structure due to the small rate of disproportional reaction at temperatures of 400-500 °C, which make possible to obtain pure Fe nanoparticles.

The increase in the gas flow rate decreases particle size and leads to the changes in particle phase

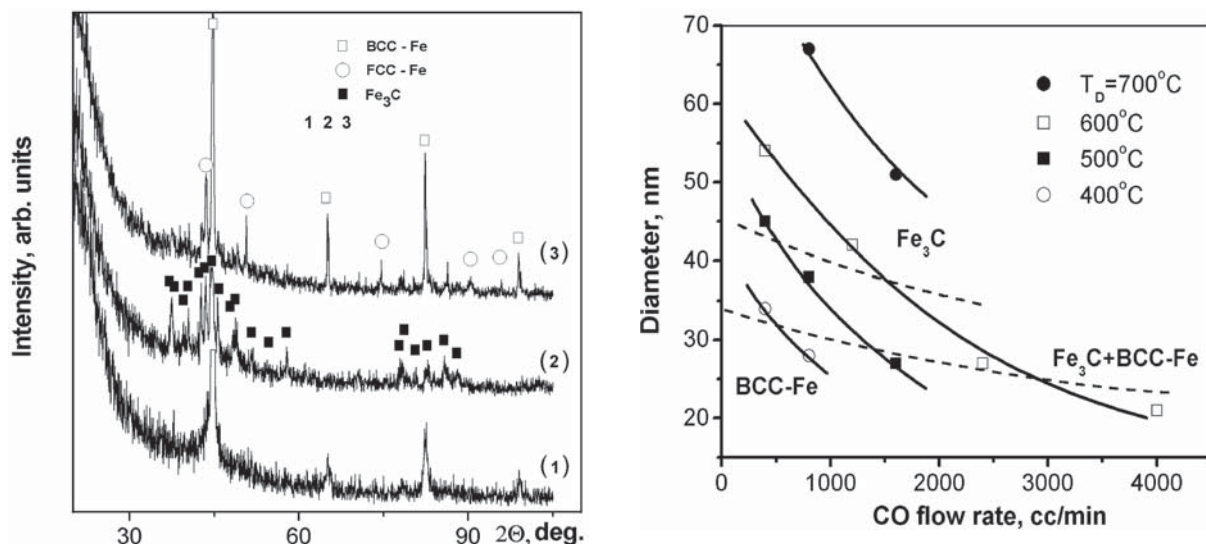


**Fig. 2.** X-ray diffraction patterns of Fe/C nanoparticles (a) and median particle diameter versus CO gas flow rate at different temperatures (b). Phase composition: FCC-Fe+BCC-Fe+Fe<sub>3</sub>C (3); Fe<sub>3</sub>C (2); and BCC-Fe (1).

composition. Fully iron particles with BCC structure were formed at the gas flow rate of 40 (400 °C), 80 (500 °C), and 200 (600 °C). Figs. 2a and 2b show X-ray diffraction patterns and mean particle size vs. decomposition/reaction temperature and CO flow rate. The reaction time (residential time in furnace) is not enough for reaction between Fe and carbon with cementite formation at the high gas flow rate. In that case, as-formed particles also have smaller size. At higher decomposition temperatures, the lines from FCC and BCC iron are observed in the X-ray diffraction pattern.

### 3.3. Fe/N nanoparticles

The Fe/N nanoparticles with a dark gray appearance exhibit different sizes in the nanometer range and are very uniform in size and shape. The contrast in the micrograph can clearly show that these nanoparticles have a core-shell type structure with a nearly spherical shape. The dark core is composed of iron nitride, while XPS data indicate that the light outer shell mainly contains iron and oxygen, although there is no iron oxide peak in the corresponding XRD pattern of this sample (Fig. 3). X-ray diffraction patterns of the as-prepared nanoparticles show that the iron nitride nanoparticles were synthesized over the temperature range of 450–1000 °C at 60 sccm NH<sub>3</sub> as a carrier gas cooled in air. From the analysis of magnetic properties, we conclude that f.c.c.  $\gamma$ -FeN<sub>x</sub> and/or  $\gamma$ -Fe(N)

nanoparticles mixed with a small amount of ferromagnetic iron nitride are obtained the decomposition temperature increased up to 1000 °C. f.c.c.  $\gamma$ -Fe(N) nanoparticles and a small amount of  $\alpha$ -Fe were prepared at 1100 °C though there is no sharp peak of  $\alpha$ -Fe. Note that when the Fe/N nanoparticles were produced under the same experimental condi-

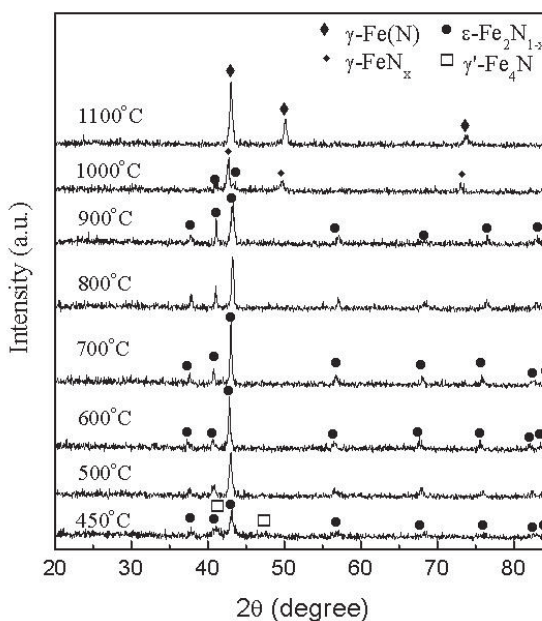


**Fig. 3.** XRD patterns of Fe/N nanoparticles synthesized at different temperatures and condensed in an air atmosphere at room temperature.

tions except using an Ar atmosphere instead of the air atmosphere, f.c.c  $\gamma$ -FeN<sub>x</sub> (and/or  $\gamma$ -Fe(N)) was replaced by  $\epsilon$ -phase of iron nitride nanoparticles at 1000 °C. However, both in an air and in Ar,  $\gamma$ '-Fe<sub>4</sub>N and  $\epsilon$ -iron nitride were obtained at 450 °C. One can conclude from XRD patterns that the strongest peak of  $\epsilon$ -phase of iron nitride condensed both in an air atmosphere and Ar atmosphere shows a shift at increasing decomposition temperature, which is caused by the different nitrogen concentrations in the Fe/N nanoparticles.

To investigate the magnetic properties of Fe/N nanoparticles, vibrating sample magnetometer experiments were conducted. It is clear that the saturation magnetizations of the Fe/N samples condensed in Ar atmosphere are higher than those condensed in air atmosphere, which may be attributed to a combination of geometric factors (shape, size and fill factors), surface factors, and different amounts of iron oxides. A small angle neutron scattering study demonstrated that nanocrystalline Fe consists of ferromagnetic Fe cores and non- or weak-magnetic interfaces [15], indicating that the disorder in the structure near the interfaces provided less magnetic moment than that of the ferromagnetic core regions. The detrimental effect of interfaces on saturation magnetization increases with decreasing particle size since the volume fraction of the interfaces increases rapidly. The saturation magnetization and coercivity of the sample prepared at 450 °C in an Ar atmosphere are 99.65 emu/g and 384.7 Oe, respectively, for the existence of  $\gamma$ '-Fe<sub>4</sub>N nanoparticles. With the decomposition temperature increasing from 450 °C to 600 °C, some paramagnetic  $\epsilon$ -phase is formed, which results in the decrease of the magnetic properties. However, with increasing the decomposition temperature from 700 °C to 1000 °C, a new equilibrium of nitrogen can be occurred between the core and the circumstance during the formation process and the new ferromagnetic  $\epsilon$ -iron nitride can be produced. The saturation magnetization of the Fe/N nanoparticles increases from 12.89 emu/g obtained at 600 °C to 127.7 emu/g obtained at 1000 °C. The coercivity of these samples increases from 146.1 Oe obtained at 600 °C to 509 Oe at 800 °C and then reduces to 393.5 Oe obtained at 1000 °C. The values of  $M_s$  of the  $\epsilon$ -Fe<sub>3</sub>N nanoparticles prepared at 900 and 1000 °C are close to or little higher than the reported bulk value of 123 emu/g [16]. Compared with the acicular Fe<sub>3</sub>N powders (about 0.8  $\mu$ m length and 0.07  $\mu$ m diameter in average dimensions) with higher magnetic properties of 135 emu/g and 540 Oe, respectively [17], our nanoparticles with small particle sizes and nearly spherical shape

weaken the contribution of shape anisotropy to magnetic properties, especially to the coercivity field. When the decomposition temperature gets to 1100 °C, the pyrolytic decomposition of the product occurs. Paramagnetic  $\gamma$ -Fe(N) (and/or  $\gamma$ -FeN<sub>x</sub>) and a small amount of ferromagnetic  $\alpha$ -Fe can be formed. Due to the phase transformation, the magnetic properties decrease rapidly. Compared with the saturation magnetization of these Fe/N nanoparticles condensed in air and Ar atmospheres, the coercivity in both systems exhibits a small difference, which is mainly attributed to some factors, like the phase compositions, the amount of the ferromagnetic components, particle size and morphologies of small isolated particles as well as surface/interface exchange effect.

#### 4. CONCLUSIONS

Fe, Fe/C and Fe/N nanoparticles were successfully synthesized by CVC process using iron pentacarbonyl as a precursor under Ar, He, CO and NH<sub>3</sub> atmosphere. The synthesized particle was nearly spherical shaped and core-shell type structure. Average particle size increases and size distribution becomes wider and more asymmetric with increasing the decomposition temperature. With the carbon potential of carrier gas increase, the resulting main phase shifted from  $\alpha$ -Fe to Fe<sub>3</sub>C. XRD analysis and magnetic properties indicate that Fe/N nanoparticles with a formula of  $\epsilon$ -Fe<sub>2</sub>N<sub>1-x</sub> ( $0 < x < 0.33$ ) are affected strongly by the experimental parameters, such as decomposition temperature and the cooling atmosphere. The magnetic measurements by VSM show the maximum value of the coercivity up to 509 Oe for the Fe/N nanoparticles prepared at 800 °C in an Ar atmosphere.

#### ACKNOWLEDGEMENT

This research was performed with the financial support of the Center for Nanostructured Materials Technology under the 21st Century Frontier R&D International Cooperation Program of the Ministry of Science and Technology, Korea.

#### REFERENCES

- [1] L. Brus // *Appl. Phys. A* **53**(1991) 465.
- [2] L. N. Lewis // *Chem. Rev.* **93**(1993) 2693.
- [3] Z. L. Wang, *Characterization of Nanophase Materials. Germany* (Wiley-VCH Verlag GmbH, D-69469 Weinheim, Germany, 2000).

- [4] X. L. Dong, Z. D. Zhang, S. R. Jin and B. K. Kim // *J. Magn. Magn. Mater.* **210** (2000) 143.
- [5] Y. D. Kim, J. Y. Chung, J. Kim and H. Jeon // *Mater. Sci. Eng. A* **291**(2000) 17.
- [6] X. G. Li, T. Murai, T. Saito and S. Takahashi // *J. Magn. Magn. Mater.* **190** (1998) 277.
- [7] H. Hahn and R. S. Averback // *J. Appl. Phys.* **67** (1990) 1113.
- [8] C. J. Choi, O. Tolochko and B. K. Kim // *Mater. Letter* **56** (2002) 289.
- [9] X. L. Dong, C. J. Choi and B. K. Kim // *J. Appl. Phys.* **92** (2002) 5380.
- [10] W. Chang, G. Skandan, S.C. Danforth and B. Kear // *Nanostructured Mater.* **4** (1994) 507.
- [11] C.J.Choi, X.L.Dong and B.K.Kim // *Scripta Mater.* **44** (2001) 2225.
- [12] K.K.Fung, B.Qin and X.X.Zhang // *Mater. Sci. and Engineering* **A286** (2000) 135.
- [13] *Fine Particles – Synthesis, Characterization and Mechanism of Growth*, ed. by T. Sugimoto (Marcel Dekker Inc., New York-Basel, 1996).
- [14] L.A. Panjushin and Yu. P. Smirnov, *Laboratory practical works on theory of metallurgy processes* (Leningrad: LPI, 1988), in Russian.
- [15] W. Chang, 31. W. Wagner, A. Wiedenmann, W. Petry, A. Geibel and H. Gleiter // *J. Mater. Res.* **6** (1991) 2305.
- [16] M. Robbins and J. G. White // *J. Phys. Chem. Solids* **25** (1964) 717.
- [17] Z. Q. Yu, J. R. Zhang and Y. W. Du // *J. Magn. Magn. Mater.* **159** (1996) L8.